Electrical Conductivities of Natural Graphite Crystals

W. Primak and L. H. Fuchs

Chemistry Division, Argonne National Laboratory, Lemont, Illinois

The principal electrical conductivities (σ_a in the basal plane and σ_c perpendicular to the basal plane) of graphite crystals isolated from several North American marbles were studied. By means of measurements of potential distributions on the surfaces of crystals carrying electric current, it was conclusively shown that σ_a/σ_c for these crystals is about several hundred at room temperature. By direct measurement σ_a was found to be $(2.6\pm0.2)\times10^4$ (ohm cm)$^{-1}$ and σ_c to vary from 150 to 230 (ohm cm)$^{-1}$ (±20 percent) at room temperature. Below room temperature it was found for two crystals that σ_a increased slowly to liquid nitrogen temperatures, then followed a T^{-1} law to about 15°K, and again slowly increased in the region 15°K to 4.2°K. Two other crystals for which σ_c was measured at low temperatures did not behave alike. For both, σ_c decreased as the temperature was lowered, reached a minimum above liquid nitrogen temperatures, and then started increasing, the one showing a T^{-1} behavior, the other increasing more slowly. For both, the rate of increase declined markedly in the region 15°K to 4.2°K.

INTRODUCTION

A NUMBER of determinations of the electrical conductivities of graphite have been reported.[1-10] The list of references is not intended to be exhaustive, and some of the determinations were incidental to other work.

The large anisotropy of the electrical conductivities of graphite was noted by Washburn,[3] who found the conductivity in the basal plane to be about 200 times the conductivity perpendicular to the basal plane. The principal conductivities of graphite will here be designated σ_a parallel to the basal plane and σ_c perpendicular to the basal plane (their reciprocals, ρ_c, ρ_a) and the square root of their ratio $(\sigma_a/\sigma_c)^{\frac{1}{2}}$ as $\mathfrak{r}$. The distribution of potentials V in such a conductor in the steady state is

$$\sigma_a[(\partial^2V/\partial x^2)+(\partial^2V/\partial y^2)]+\sigma_c(\partial^2V/\partial z^2)=0.$$

If the substitution $\zeta=\mathfrak{r}z$ be made, then

$$(\partial^2V/\partial x^2)+(\partial^2V/\partial y^2)+(\partial^2V/\partial\zeta^2)=0,$$

the potential distribution being similar to that in an isotropic body of the same dimensions in the directions of the basal plane, but $\mathfrak{r}$-fold larger perpendicular to it. Since most graphite crystals available for measurement are perhaps 1/10 to 1/20 as thick as their average diameter, their equivalent isotropic bodies are small blocks. The usual assumptions in electrical conductivity measurements, that the current is spread uniformly in the region between the potential probes, may not here

be justified, and the proper method of determining the electrical conductivities is to study the potential distributions on the surfaces of crystals conducting current and to apply the appropriate solution of Laplace's equation.

GRAPHITE CRYSTALS

Recently Krishnan and Ganguli,[7] and later Dutta,[8] have reported measurements indicating $\mathfrak{r}^2\cong10^4$. Since their results are quite different from the results reported by others working with different specimens, it is considered desirable to carefully describe the crystals which were used in the present measurements and to give their source. All of the crystals used in the present measurements were isolated from graphite-bearing marbles. One specimen of marble collected from the Ticonderoga, New York area was furnished by Professor C. Palache (Harvard University). Another specimen was supplied by Mr. H. S. Spence (Department of Mines and Resources, Canada) and was labelled Bouthillier Township, Labelle County, Quebec. A specimen from Crown Point, New York was secured from Ward's Natural Science Establishment, Rochester, New York. Most of the elongated crystals on which σ_a was measured were isolated from a boulder found by the authors at the Lead Hill Mine, Ticonderoga, New York, a fortunate find in the mine tailings, most of which were of a different character.

The crystals were isolated in the following manner. The calcite was dissolved in dilute hydrochloric acid. The insoluble residue was then treated alternately with concentrated hydrochloric and hydrofluoric acids on a steam bath for some weeks until all the minerals but graphite were rendered soluble and washed away with distilled water.[11] Some of the crystals were loaded into a graphite capsule and heated to 3000°C in a graphite tube furnace swept with helium which in some runs, during part of the heating, bore CCl_4 vapor. Typical spectrochemical analyses before and after such heatings

[1] D. E. Roberts, Ann. Physik (4) 40, 453 (1913); Phil. Mag. 26, 159 (1913).

[2] J. Koenigsberger and J. Weiss, Ann. Physik 35, 2 (1911).

[3] G. E. Washburn, Ann. Physik (4) 48, 236 (1915).

[4] W. J. de Haas and P. M. Van Alphen, Proc. Natl. Acad. Amsterdam 34, 70 (1931).

[5] Meissner, Franz, and Westerhop, Ann. Physik 13, 555 (1932).

[6] E. Ryschkewitz, Z. Elektrochem. 29, 474 (1923).

[7] K. S. Krishnan and N. Ganguli, Nature 144, 667 (1939).

[8] A. K. Dutta, Phys. Rev. 90, 187 (1953).

[9] Grisdale, Pfister, and Van Roosbroeck, Bell System Tech. J. 30, 292 (1951).

[10] G. H. Kinchin, Proc. Roy. Soc. (London) A217, 9 (1953).

[11] This method of treatment was devised by G. Hennig of this laboratory.

are given in Table I. No difference in the electrical conductivities between heated and unheated crystals was noted.

From among a very large number of graphite crystals, most of them too imperfect to use, there were found a few suitable for the measurements described here. The appearance of some of these crystals is shown in Fig. 1. The prominent striae are reflections from zones twinned in the manner described by Palache.[12] Since the crystals are continuous across the twin plane, and since the zones are large compared to the mean free path of electrons in a solid, it is assumed that the gross twinning would have only a small effect on the electrical con-

FIG. 1. Photomicrograph of typical graphite crystals of the sort used in the measurements described here. The scale is millimeters.

TABLE I. Typical spectrum analysis of natural graphite crystals before and after purification.

Element analyzed for	Before purification (ppm)	After purification (Case I—without CCl_4) (ppm)	After purification (Case II—with CCl_4) (ppm)
Ag	<0.1	<0.1	<0.1
Al	1000	<5	<10
As	100	<20	<10
B	20	3	1
Ba	10	<2	<5
Be	<0.5	<0.5	<0.5
Bi	<0.2	<0.2	<0.5
Ca	100	<2	<10
Co	<2	<2	<5
Cr	<1	<1	<1
Cu	10	<1	<1
Fe	2000	<1	2
Hg	<5	<5	<1
K	<10	<10	<20
Li	<1	<1	<1
Cd	<100	<100	
Mg	2000	<0.5	<0.5
Mn	0.5	<0.1	<0.2
Na	50	<2	5
Ni	10	<1	<2
P	<50	<50	<20
Pb	15	<0.5	<1
Sb	<1	<1	<1
Si	30	<2	<5
Sn	10	<5	<5
Sr	<10	<10	<10
Ti	<1	<1	<2
V	<1	25	<2
Zn	<20	<20	<20
Zr	<10	<10	<5

ductivities. The more circular crystals were used for determining σ_c and in one method of determining r, while the elongated ones were used in determining σ_a and in another method for determining r.

The dimensions of a crystal were determined by measuring the area of the basal plane with a binocular microscope fitted with a net reticule ocular calibrated against a stage micrometer. The crystal was then weighed and its mean thickness computed from its area and an assumed density of 2.265. The densities of a number of crystals were determined by a flotation method and found to vary between 2.262 and 2.268.[13]

[12] C. Palache, Am. Mineralogist 27, 713 (1941).
[13] We are indebted to Paul Day of this laboratory for making these measurements.
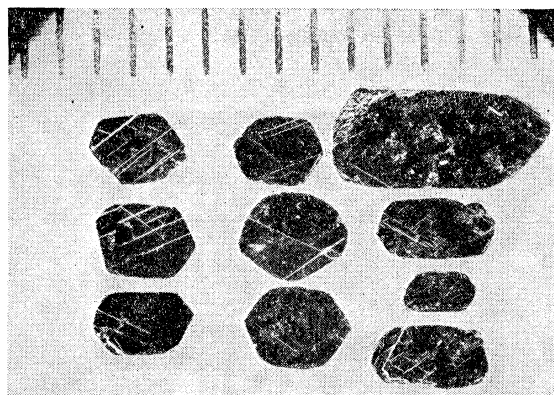
Some of the thicknesses were checked using a microscope fitted with a filar micrometer.

ELECTRICAL MEASUREMENTS

The methods used in making the electrical measurements were the following. Two sets of contacts were established to the crystal, current electrodes and potential probes, which were not in contact with each other. Thus, in all cases, the potential drops which were measured were potential drops on the surface of the graphite and did not include potential drops across contact resistances. The current was measured by the potential drop across a standardized resistor in series with the current contacts. Since both the current and potential drop were measured in succession with the same potentiometer, the use of a carefully calibrated standard cell was obviated. The potential drops across the standard resistor were large, hence no correction for contact potentials was necessary. The potential drops across the potential probes were often small, necessitating such a correction. It was occasionally made by subtracting the potential drop with the current off
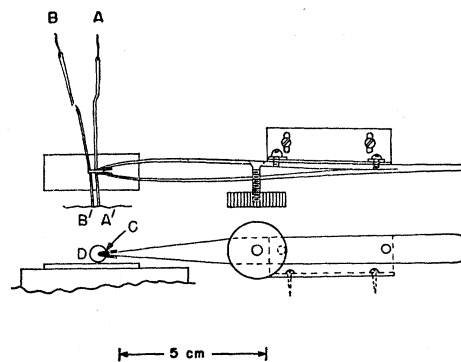
FIG. 2. Apparatus used to determine r shown with mercury-filled capillaries for electrodes and probes. A and A' are the current electrodes; B and B' are the potential probes (they were held with micromanipulators); C are insulating pads of mica held to the forceps with glyptal varnish; D is the graphite crystal.
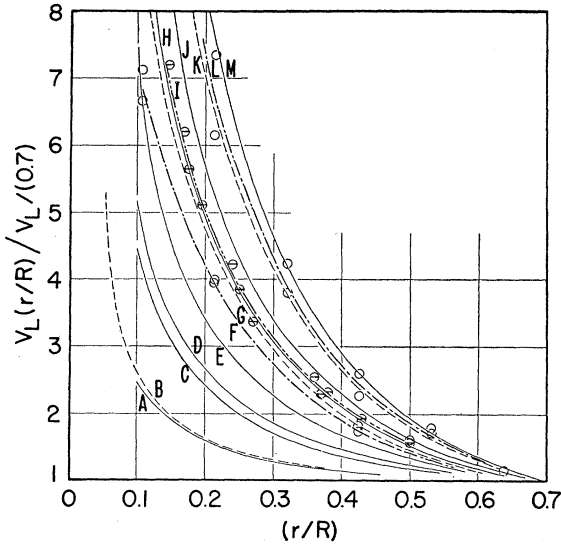
FIG. 3. Graphs of $V_L(r/R)/V_L(0.7)$. The solid curves are calculated for R/L: $A=0.159$, $C=0.333$, $D=0.385$, $E=0.556$, $H=0.714$, $J=0.769$, $M=1.00$. The dashed curves are measured for isotropic bars of R/L: $B=0.172$, $G=0.694$, $K=0.917$. The heavy dot-dash curves are results for: F, graphite crystal $23R$, I, crystal $6R$, L, crystal $20R$.

from the potential drop with the current on, or occasionally by reversing current and potentiometer leads and taking the average of the two potential drops. The correction was found to be about the same by either method, usually about 2 to 10 microvolts. Three types of apparatus were used and are shown in Figs. 2, 4, and 9. The first was used to measure $\mathfrak{r}$, the second to measure $\mathfrak{r}$ and σ_a, the third to measure σ_c.
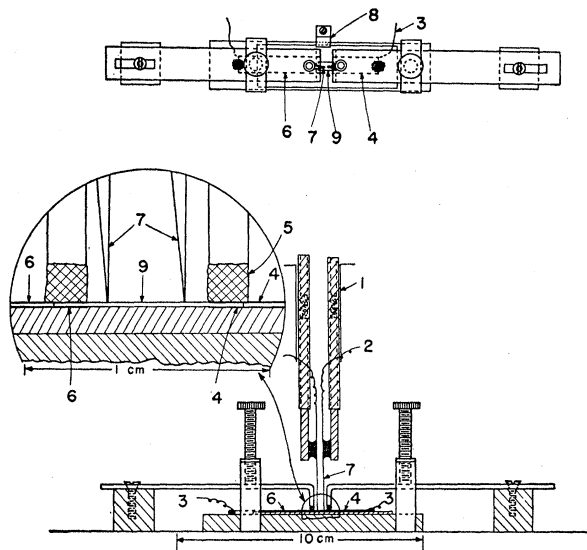
FIG. 4. Apparatus used to determine σ_a and $\mathfrak{r}$. 1. Micromanipulator support arm. 2. Potential lead. 3. Current lead. 4. Movable gold foil current electrode (attached to movable glass plate). 5. Rubber foot. 6. Fixed gold foil current electrode (attached to plastic base). 7. Tungsten wire potential probe. 8. Clamp for glass plate. 9. Graphite crystals.

The Determination of $\mathfrak{r}$

The arrangement of the apparatus is shown in Fig. 2 and is essentially that of a finite cylinder carrying electric current to which contact is made by means of small electrodes placed at the center of the bounding circular faces. Laplace's equation for the equivalent isotropic body is here

$$\frac{\partial^2 V}{\partial r^2} + \frac{1}{r}\frac{\partial V}{\partial r} + \frac{\partial^2 V}{\partial \zeta^2} = 0,$$

where r is the radius variable. The boundary conditions and the solution for this case are discussed by Gray et al.[14] The potential at any point in the equivalent isotropic cylinder (radius R; length λ) is

$$V = \frac{S}{\pi\sigma_a(\lambda/2)} \sum_{n=1}^{\infty} \sin\frac{n\pi}{2}\sin\frac{n\pi\zeta}{\lambda}$$
$$\times \left[K_0\left(\frac{n\pi r}{\lambda}\right) + \frac{K_1(n\pi R/\lambda)}{I_1(n\pi R/\lambda)} I_0\left(\frac{n\pi r}{\lambda}\right) \right],$$

where S is the current and $V=0$ at the midplane. In this experiment the potential probes were located at $\zeta=\pm\lambda/2$ and moved so that they were at equal distances from the respective current electrode on that face. The potential drop measured V_L was thus twice the value obtained by setting $\zeta=\lambda/2$. Remembering that the thickness of the crystal $L=\lambda/\mathfrak{r}$,

$$V_L = \frac{4S}{\pi L\mathfrak{r}\sigma_a} \sum_{n=1}^{\infty} \sin^2\frac{n\pi}{2}\left[K_0\left(n\pi\frac{R}{\mathfrak{r}L}\frac{r}{R}\right) \right.$$
$$\left. + \frac{K_1\left(n\pi\frac{R}{\mathfrak{r}L}\right)}{I_1\left(n\pi\frac{R}{\mathfrak{r}L}\right)} I_0\left(n\pi\frac{R}{\mathfrak{r}L}\frac{r}{R}\right) \right].$$

The function $V_L(r/R)$ was computed for a number of values of $R/\mathfrak{r}L$. In Fig. 3 is plotted $kV_L(r/R)$, the constant k being chosen to make the function unity at $r/R=0.7$. These curves are shown by the solid lines on the graph. The potentials similarly adjusted across the faces of a number of metal bars (presumed isotropic, $\mathfrak{r}=1$) of various dimensions, whose R/L varied from 1.09 to 34.9, were determined and were found to match the computed curves very nicely. The results for three Monel bars whose respective radii/length ratios were 1.743/1.901, 1.745/2.508, and 1.745/10.16 are shown in the figure as dashed lines; another, 1.745/5.09, fell so close to one of the computed curves, $R/L=0.333$, that

[14] Gray, Mathews, and Macrobert, Bessel Functions (Macmillan and Company, Ltd., London, 1931), pp. 143, 146, and 147.

it is omitted. The adjusted potentials obtained for three of the graphite crystals which were measured are plotted in the figure as circles and are joined by a heavy dot-dash line. From the position of one of these curves on the graph, the value of R/rL for the crystal can be read off; and by introducing its dimensions, r is obtained directly. To insure comparable experimental potentials, the current was measured at each setting of the potential probes, and the potentials chosen for adjustment were the measured potentials divided by the measured currents.

For the machined bars, the current electrodes were machined pins or fine needles, and the potential probes were fine needles. Their positions were measured with comparators reading to 0.01 mm. The measurements on the crystals could not be made as precisely. Here mercury drops held by capillary tubes or on amalgamated copper wires seemed to make the best electrodes and probes. The sizes of the electrodes and probes were relatively much larger than those used for the bars.

TABLE II. Determination of r by the ratio apparatus.

Crystal	Radius (cm)	Thickness (L) (cm)	r
2R (Quebec)	0.163	0.013	20
6R (Quebec)	0.210	0.014	21
7R (Crown Point)	0.126	0.0086	19
8R (Crown Point)	0.118	0.0045	25
12R (Quebec)	0.136	0.0088	21
20RC	a	0.0104	25
24RC	a	0.0133	20–25
26RC	a	0.0243	14–17
27RC	a	0.0166	13–17
29RC	a	0.0117	~17

a These crystals were cut with a sand blast to form a circular disk of radius 0.241 cm.

The potential probe positions were measured with binocular microscopes fitted with micrometer reticule eyepieces. The crystals were somewhat irregular in shape and sometimes nonuniform in properties; hence the curve V_L for them was usually determined along several different radii. The potential curves given by some of the crystals crossed several of the family of curves shown in the figure. This might be expected very close to the electrodes. It was presumed that when it occurred some distance away, the conductivities in these crystals were not uniform and the data were therefore discarded. Several crystals were cut into a nearly perfect cylindrical shape by holding them between two metal cylinders and removing the protruding edges with a sand blast from a dental drill. The results for a number of uncut and cut crystals are given in Table II.

Confirmatory evidence for values of r in this range was obtained with the use of the apparatus shown in Fig. 4 using some of the elongated crystals. For the arrangement shown here the variables of Laplace's equation are separable in Cartesian coordinates. For
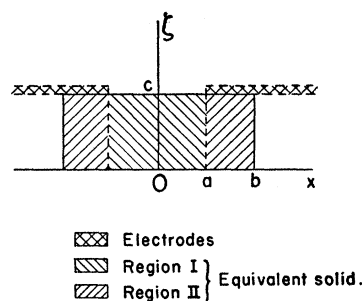
FIG. 5. Half of the equivalent isotropic solid in which the potential distribution is analyzed.

the equivalent isotropic solid

$$(\partial^2 V/\partial x^2)+(\partial^2 V/\partial \zeta^2)=0.$$

The arrangement analyzed is that of Fig. 5. In the experimental arrangement, each electrode covered about $\frac{1}{4}$ of the crystal face, and there were electrodes on both the upper and lower surfaces of the crystal. The potential drop was measured for various separations (symmetrical) of the potential probes on the upper surface (Case I). The upper electrodes were then insulated from the crystal by inserting strips of paper, and the potential drops again measured on this face (Case II). The results for two crystals are shown in Fig. 6. It is seen that in both cases the potential drop as a function of separation was linear up to distances as close to the electrodes as could be measured. What was determined in effect was $(\partial V/\partial x)$ on the upper surface and in the central plane of a hypothetical crystal of double thickness with electrodes attached at similar positions. The
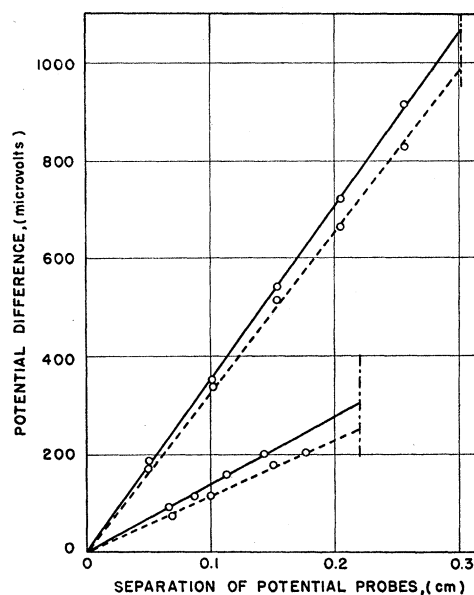
FIG. 6. Potential distribution on the faces of graphite crystals for a current of 0.098 amp. Upper curves, AX-2. Lower curves, AX-1. ——————— Case I; – – – – – – Case II; – – – – – separation of current electrodes.
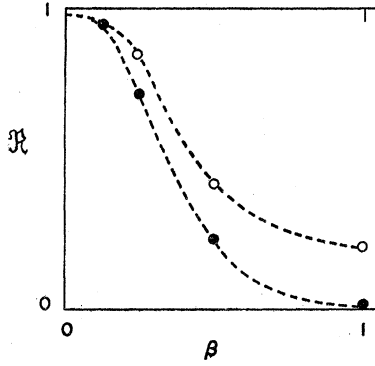
Fig. 7. $\mathfrak{R}$ as a function of β. ○ First boundary condition; ● second boundary condition.

appropriate boundary conditions for the planes $x = \pm b$ and $\zeta = 0$ are obvious; for $\zeta = c = \lambda/2$ it is not quite clear. Potential drops were measured along the gold foils in one case and found to be about 25 μv/mm for the currents which were employed. For a 2-mm overlap this is small compared to the potential drops in the surface of the graphite between the electrodes, which were between several hundred and over 1000 μv, hence the potential along the electrode was essentially constant. However, it cannot be assumed that this is true for the graphite under the electrode since the contact resistances were high: in several cases the potential drops from the gold to the graphite adjacent to the electrode were measured and found to be several thousand microvolts and were found to change for some hours after contact was established. It thus seems reasonable to believe that the correct condition for this boundary is one between the following extremes:

(1) $(\partial V/\partial x) = k_1$, a constant from 0 to a and null from a to b,

(2) $(\partial V/\partial \zeta) = k_2$, a constant from a to b and null from 0 to a;

the first boundary condition being expected to give too small a value for $(\partial V/\partial x)$ under the electrode, and the second too large a one.

The solution for the first condition[15] may be obtained by dividing the equivalent isotropic solid into two regions, as shown in Fig. 5, for which the respective potential distributions are,

$$V_{\mathrm{I}} = \sum A_n \sinh\alpha x \cos\alpha\zeta + A_0 x \quad (0 \leqslant |x| \leqslant b),$$

$$V_{\mathrm{II}} = \sum B_m \sinh\beta x \cosh\beta\zeta + B \quad (a \leqslant |x| \leqslant b).$$

Since the boundary condition at $x = \pm b$ requires m be *odd only*, it is necessary to expand the boundary condition for the upper surface in the interval 0 to $2b$. It is obvious that $\alpha = n\pi/c$ and $\beta = m\pi/2b$. It is found that

$$B_m = (8k_1 b/m^2\pi^2)(\sin\beta a/\cosh\beta c).$$

[15] This solution is due to O. C. Simpson of this laboratory.

At $x = a$, $(\partial V_{\mathrm{I}}/\partial x) = (\partial V_{\mathrm{II}}/\partial x)$; hence,

$$\sum_n \alpha A_n \cosh\alpha a \cos\alpha\zeta + A_0 = \sum_{m\,\mathrm{odd}} \beta B_m \cos\beta a \cosh\beta\zeta.$$

The final result desired, $(\partial V_{\mathrm{I}}/\partial x)$, is obtained by expanding

$$\cosh\beta\zeta = \sum_n D_n \cos\alpha\zeta + D_0/2,$$

when it is found that

$$D_n = (2m/\pi)\{(2b/c)\cos n\pi/[m^2 + n^2(2b/c)^2]\}\sinh\beta c.$$

Thus,

$$\sum \alpha A_n \cosh\alpha a \cos\alpha\zeta + A_0 = \sum_{m\,\mathrm{odd}} \sum_n \beta B_m \cos\beta a D_n^m \cos\alpha\zeta.$$

Hence,

$$A_0 = \sum_{m\,\mathrm{odd}} \frac{2k_1}{m^2\pi^2}\frac{2b}{c}\sin\beta a \tanh\beta c \equiv \frac{2k_1}{\pi^2}\frac{2b}{c}\Sigma_1.$$

Thus,

$$2k_1 = \pi^2(c/2b)(A_0/\Sigma_1),$$

and

$$A_n = \frac{2c\cos n\pi}{\pi\cosh\alpha a}\frac{A_0}{\Sigma_1}\sum_{m\,\mathrm{odd}}\frac{\sin 2\beta a \tanh\beta c}{m^2 + n^2(2b/c)^2}$$

$$\equiv \frac{2c\cos n\pi}{\pi\cosh\alpha a}\frac{A_0\Sigma_2}{\Sigma_1}.$$

Since $\mathrm{grad}V = (\partial V_{\mathrm{I}}/\partial x)$ at $x = 0$, the half-current S is

$$S = (\sigma/\mathfrak{r})\int_0^c (\partial V_{\mathrm{I}}/\partial x)_{x=0}dy,$$

where σ is σ_a multiplied by the depth of the crystal, and where the factor $1/\mathfrak{r}$ appears because it is necessary to pass an $\mathfrak{r}$-fold greater current in the equivalent isotropic body to maintain the same potential drop as in the graphite crystal. Then

$$S = \sigma A_0 c/\mathfrak{r} \quad \mathrm{and} \quad A_0 = \sigma S\mathfrak{r}/c.$$

Finally,[15]

$$\frac{(\partial V_{\mathrm{I}}/\partial x)}{S} = \frac{1}{\sigma c/\mathfrak{r}}\left[1 + \sum_n \frac{2n\cos n\pi}{\cosh(n\pi a/c)}\right.$$

$$\left. \times \frac{\Sigma_2}{\Sigma_1}\cosh\frac{n\pi x}{c}\cos\frac{n\pi\zeta}{c}\right].$$

Table III. Approximate values of $\mathfrak{r}$ from a-axis apparatus.

Crystal[a]	Length (2b) (cm)	Half-thickness (L/2) (cm)	$\mathfrak{R}$ (experimental)	Boundary condition 1		Boundary condition 2	
				$\frac{1}{2}\lambda/2b$	$\mathfrak{r}$	$\frac{1}{2}\lambda/2b$	$\mathfrak{r}$
AX-1	0.61	0.050	0.83	0.27	33	0.21	26
AX-2	0.57	0.0045	0.91	0.22	28	0.17	22
AX-3	0.325	0.00377	0.92	0.20	17	0.16	14

[a] These were all Ticonderoga crystals collected by the authors.

Then for Case I and Case II, respectively,

$$\left[(\partial V_I/\partial x)/2S\right]_I=(\mathfrak{r}/\sigma\lambda)\left[1+\sum_n\frac{2n}{\cosh(n\pi 2a/\lambda)}\frac{\Sigma_2(\lambda/2)}{\Sigma_1(\lambda/2)}\right],$$

$$\left[(\partial V_I/\partial x)/S\right]_{II}=(\mathfrak{r}/\sigma\lambda)\left[1+\sum_n\frac{2n\cos n\pi}{\cosh(n\pi a/\lambda)}\frac{\Sigma_2(\lambda)}{\Sigma_1(\lambda)}\right].$$

The ratio $\mathfrak{R}=\left[(\partial V_I/\partial x)/S\right]_{II}/\left[(\partial V_I/\partial x)/2S\right]_I$ can be used to determine λ and hence $\mathfrak{r}$.

The solution for the second boundary condition follows in a much simpler manner. The boundary conditions are satisfied by

$$V=\sum_{m\,odd}C_m\cosh\beta\zeta\,\sin\beta x,$$

where the boundary condition for the upper surface is again expanded in the interval 0 to $2b$ and it is found that

$$C_m=(8bk_2/m^2\pi^2)(\cos\beta a/\sinh\beta c),$$

where $k_2=(\partial V/\partial y)$ under the electrodes. The half-current is

$$S=(\sigma/\mathfrak{r})\sum C_m\sinh\beta c,$$

and for this boundary condition

$$\left[\frac{(\partial V/\partial x)}{2S}\right]_I=-\frac{\mathfrak{r}}{\sigma}\frac{\pi}{4b}\sum_{m\,odd}\frac{1}{m}\frac{\cos(m\pi a/2b)}{\tanh(m\pi\lambda/4b)}\Big/$$

$$\sum_{m\,odd}\frac{1}{m^2}\cos(m\pi a/2b),$$

$$\left[\frac{(\partial V/\partial x)}{S}\right]_{II}=-\frac{\mathfrak{r}}{\sigma}\frac{\pi}{2b}\sum_{m\,odd}\frac{1}{m}\frac{\cos(m\pi a/2b)}{\sinh(m\pi\lambda/2b)}\Big/$$

$$\sum_{m\,odd}\frac{1}{m^2}\cos(m\pi a/2b).$$

For most of the measurements a/b was about $\frac{1}{2}$. Using this value, $\mathfrak{R}$ was computed for several values of $0.5\lambda/2b$. The function is sketched in Fig. 7. Since $\lambda=\mathfrak{r}L$, a determination of $\mathfrak{R}$ experimentally can, with

TABLE IV. Values of σ_a/δ for graphite crystals.

Crystal	Thickness (L) (cm)	Depth (cm)	Length $(2b)$ (cm)	Current $(2S)$ $(10^{-2}$ amp)	$\partial V/\partial x$ $(10^{-6}$ volt/cm)	σ_a/δ $(10^4$ (ohm cm)$^{-1})$
AX-1	0.0101	0.326	0.61	9.86	200/0.144	2.16
AX-2	0.00445	0.257	0.53	9.83	723/0.205	2.49
AX-3	0.00743	0.095	0.33	9.80	604/0.115	2.65
2A	0.016	0.185	0.33	9.69	158/0.134	2.8
3A	0.00433	0.285	0.41	9.68	370/0.120	2.6
4A	0.0127	0.28	0.51	9.72	184/0.188	2.8
8A	0.0110	0.356	0.51	9.70	152/0.164	2.7
9A	0.0057	0.185	0.46	9.62	691/0.213	2.8
10A	0.0136	0.206	0.443	9.93	219/0.170	2.69
12A	0.0122	0.210	0.426	9.80	571/0.169	2.50
13A	0.0171	0.200	0.378	9.93	223/0.178	2.41
17A	0.0062	0.215	0.619	9.77	880/0.298	2.42
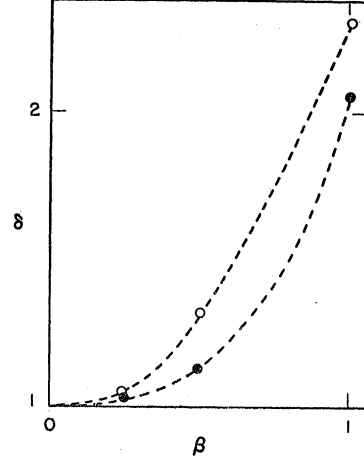
FIG. 8 δ as a function of β. ○ First boundary condition; ● second boundary condition.

this curve, give an approximate value of $\mathfrak{r}$. The results for three crystals are given in Table III.

The Value of σ_a

If electrodes were placed on the faces of the graphite crystal corresponding to $x=\pm b$ (Fig. 5), the potential gradient along x divided by the half current would be

$$(\partial V/\partial x)/S=2/\sigma L=\mathfrak{r}/\sigma c.$$

With the experimental arrangement used in the preceding experiment Case I, according to the first boundary condition, the potential gradient per unit half-current at $\zeta=c$, $x=0$ is greater than this by the factor δ_1,

$$\delta_1=1+\sum_n\frac{2n}{\cosh(n\pi a/c)}\frac{\Sigma_2(c)}{\Sigma_1(c)},$$

while for the second boundary condition it is greater by the factor δ_2,

$$\delta_2=\frac{\pi c}{2b}\frac{\sum_{m\,odd}(1/m)[\cos(m\pi a/2b)/\tanh(m\pi c/2b)]}{\sum_{m\,odd}(1/m)[\cos(m\pi a/2b)]}.$$

The factors were computed for several values of $c/2b$ under the assumption that $a/b=\frac{1}{2}$ and are shown in Fig. 8. The correct factor δ may be presumed to lie between δ_1 and δ_2. The value of σ_a/δ was determined for a number of crystals, and the results are given in Table IV.

For crystals AX-1, AX-2, and AX-3 the value of δ was in fact determined by the determination of $\mathfrak{R}$ and $0.5\lambda/2b$ and by referring to Fig. 8 it can be seen that for these crystals $\delta<1.03$. For the thickest crystals, 2 A, 13 A, 10 A, and 12 A, δ would not be larger than 1.15. It is therefore concluded that for these crystals $\sigma_a\cong 2.6(10^4)$ (ohm cm^{-1}) within 10 percent.
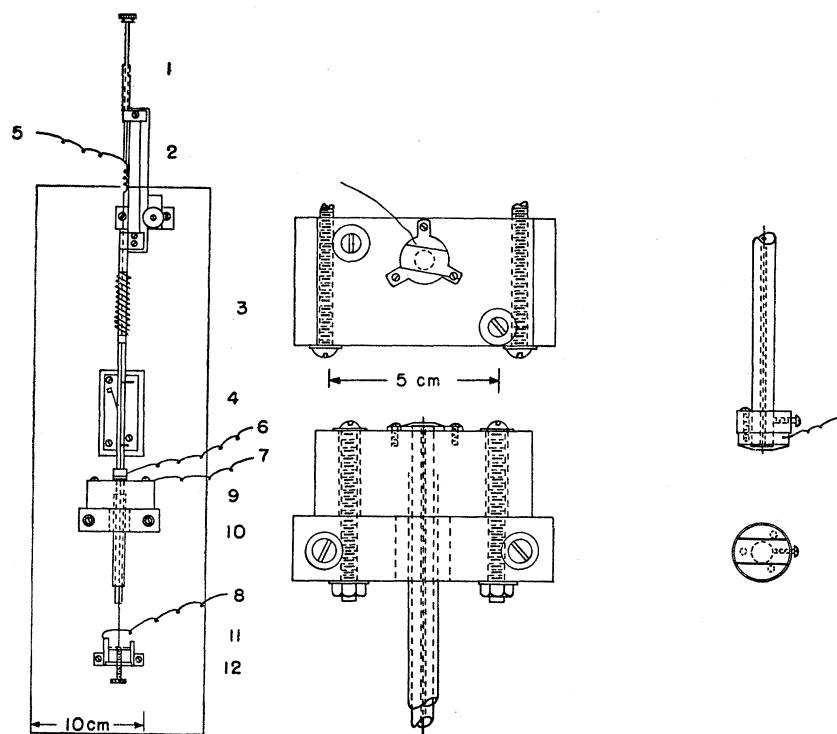
FIG. 9. Apparatus used to determine σ_c. 1. Friction adjustment for upper potential probe. 2. Rack and pinion adjustment for upper current contact. 3. Spring to regulate current contact pressure. 4. Alignment block for upper current contact. 5. Potential lead. 6. Upper current contact lead. 7. Lower current contact lead. 8. Lower potential lead. 9. Lower current contact block. 10. Support platform for current contact block. 11. Cantilever spring for lower potential probe. 12. Withdrawing screw for lower potential probe. Details of upper and lower contacts are shown.

The Determination of σ_c

The apparatus shown in Fig. 9 was used to determine σ_c. A plastic mask prepared for each crystal served to prevent the gold foils from overlapping the edges of the crystal. Potential probes of 2-mil gold wire were brought to the crystal faces through a No. 80 hole (0.014 in.) drilled through the rubber and the gold foil. In the early measurements, the gold foils were strips to which contact was made at one end. It was observed that an appreciable potential drop occurred along these strips. In the apparatus shown here the gold foils are cut in the form of a disk and soldered to a heavy copper ring at a number of points to minimize this effect. The arrangement should give rise to a nearly

linear current flow through the crystal. The only question which arises concerns the distribution of potential about the hole. The problem is complicated by the large and somewhat variable contact resistance between the gold and the graphite, perhaps some tenfold greater than the resistance of the crystal itself. It was therefore considered desirable to explore these potentials experimentally.

An apparatus was constructed in which a crystal was clamped between gold foils in a manner similar to that in the apparatus shown in Fig. 9, but with a hole drilled only in the upper plate. This hole was 0.112 cm in diameter, about $3\frac{1}{2}$ times the diameter of the hole in the apparatus used to measure σ_a. The potential drop from the center of the hole to close to the edge of the
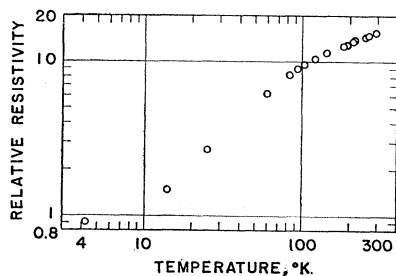
FIG. 10. Effect of temperature on the a-axis resistivity of crystal LTA-2.

TABLE V. The determination of σ_c (current about 0.1 amp).

Crystal	Resistance (10⁻⁵ ohm)	Area (cm²)	Thickness (cm)	σ_c ((ohm cm)⁻¹)
31	222	0.0563	0.0190	156
32	165	0.0816	0.0282	215
25	126	0.0714	0.0177	167
26	109	0.0870	0.0197	193
27	232	0.0387	0.0191	226
28	167	0.0677	0.0221	175
29	163	0.0620	0.0221	224
30	140	0.0642	0.0200	229
33	124	0.0502	0.0123	203

hole was measured in several directions, and the largest drop found was 4 microvolts for a current of 0.10 amp. Since the potential drops measured for most of the crystals were about 100 microvolts, it was assumed that the error introduced by the smaller hole of the σ_c apparatus was small. The results of measurements with the σ_c apparatus are given in Table V. All the measurements were made with a current of about 0.1 amp. The resistance given is the average of 6 to 10 measurements, for each of which the crystal was reinserted into the apparatus. The extreme deviations among these measurements were $\pm(10-15)$ percent.

Several reasons are suggested as contributing to the large deviations in the measurements of individual crystals. The crystals do not seem to have a uniform resistance over their entire area. In some cases it was observed that the thickness was not uniform. The contact resistances of the electrodes are high, much greater than the resistance of the crystal. If this contact resistance is not uniform, it would contribute to making the bounding planes nonequipotential. However, the
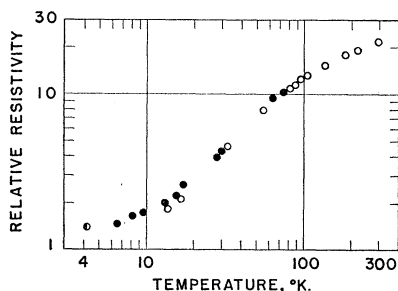
FIG. 11. Effect of temperature on the a-axis resistivity of crystal LTA-3. ○ Run 1; ● Run 2.

average of a number of determinations of a crystal seem quite reproducible. Some 42 sets of measurements on Crystal 31 made over several years, each set consisting of 8 to 10 measurements, deviate by only some 10 percent from the results of the first set, quoted here. Some evidence has accrued which indicates that σ_c does in fact vary somewhat from one crystal to another.

The Effect of Temperature on σ_a and σ_c

Apparatus similar to that shown in Figs. 4 and 9 but much more compact were constructed[16] and suspended at the ends of long Monel tubes in a meter-long 10-cm diameter Dewar which was cooled with liquid helium. After the liquid helium had evaporated, the temperature was permitted to rise slowly, and measurements of the resistances of the crystals were continued. In this manner the resistances of the crystals were determined at various temperatures from liquid helium temperature to room temperature. The temperatures were read on a copper-constantan thermocouple, the liquid helium and liquid nitrogen temperatures being taken as calibration

[16] The pads which were used to press the gold foils into contact with the crystals were made of polyvinyl chloride plastic, which seemed to behave better than rubber at low temperatures.
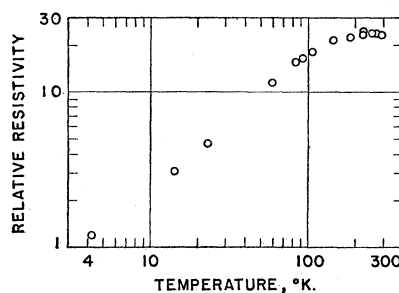
FIG. 12. Effect of temperature on the c-axis resistivity of crystal LTC-4.

points. Results for 2 a-axis crystals and for 2 c-axis crystals are shown in Figs. 10, 11, 12, and 13, where the relative resistivities are plotted as a function of temperature. The first power dependence of ρ_a on temperature from about 15°K to about 80°K seems characteristic. From these two results it would seem that ρ_c is more variable, but the maximum somewhat below room temperature seems characteristic although it seems to appear at different temperatures for different crystals. Further measurements at low temperatures are in progress.

DISCUSSION

The values found here for r determined directly from relative potential distributions are larger than the ratio of the separate measurements of $(\sigma_a)^{\frac{1}{2}}$ to that of $(\sigma_c)^{\frac{1}{2}}$ by a factor of about 1.5. It was shown that for the crystals measured here, σ_a could not have been greater by 5 percent than the values reported. It does not seem possible that σ_c could be in error by the factor required to produce agreement, 2 or 3. It must therefore be concluded that there may be small errors in σ_a and σ_c; perhaps 5 percent in σ_a and perhaps as much as 20 percent in σ_c; but that most of the error is in r and may reside in the large electrodes used in the first method and the irregular shape of the crystals in the second. In the first method the large electrodes would cause the potential to spread more uniformly over the surface and not to rise so high near the electrode; both these effects would move the potential curve to the left on adjustment, leading to a high value for r. A detailed discussion of the second method is hardly necessary; in fact a/b was never exactly $\frac{1}{2}$ as assumed, and the crystals were not exactly rectangular in the xy plane, so that the dimensions used were not exact. However, although these direct determinations do not give exact values of r, they prove conclusively that for these crystals σ_a/σ_c lies in the range 10^2 to 10^3.
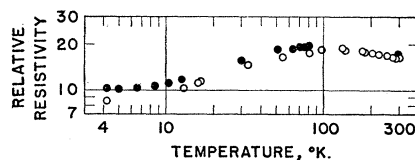
FIG. 13. Effect of temperature on the c-axis resistivity of crystal LTC-5. ○ Run 1; ● Run 2.

The results reported here for σ_a are in agreement with those given by Grisdale, Pfister, and Roosbroeck.[9] They also agree with the greater of two values reported by Kinchin[10] and with the value Roberts[1] gives for his best specimens. They are 40 to 100 percent larger than Washburn's[3] values, but this difference may be accounted for in terms of the analysis of potential distributions made here. Dutta's[8] values are about $2\frac{1}{2}$ times smaller than the ones reported here. The values for σ_c reported here are a little greater than those Washburn found for what he considered his best samples, and they are about twice as great as his average value and the value reported by Grisdale, Pfister, and Roosbroeck but are some 200 times greater than Dutta's values for σ_c. It is therefore considered that the results reported here are in agreement with the results found by others except for those of Dutta[8] and the similar fragmentary earlier report by Krishnan and Ganguli.[7] It is difficult to assess their work from the information they have published since they have not given a sufficiently detailed description of their crystals. However, several comments can be made on the basis of experiments performed by the authors and others. Ott[17] claimed that even the agitation of the acid during solution of the rock was sufficient to alter the diffraction patterns. Cleaving and cutting crystals, such as Dutta did, may be expected to affect them severely. Attempts were made by one of the authors, in collaboration with Hennig and Montet,[18] to copperplate some graphite crystals. It was found that under some conditions, the graphite swelled enormously or blistered, which was interpreted as being caused by the interlamellar penetration of protons which combine to form hydrogen gas between the planes. It was therefore concluded that copperplated graphite crystals would have to be very carefully examined before any results with them could be trusted. It further must be demonstrated that (a) copperplatings provide an equipotential surface, for an appreciable potential drop may occur along a thin copperplate, and (b) that there is no appreciable contact resistance between such a plate and the graphite surface.

It may be expected that imperfections in the crystal will introduce scattering centers and decrease the mean free path. This effect would become especially noticeable in measurements at low temperature. However, since imperfections might trap electrons or create holes, the argument is not conclusive. It was found that introducing imperfections by means of fast neutron irradiation decreased both σ_a and σ_c and both then developed a slightly negative temperature coefficient of resistivity over the range of temperatures 4.2°K to 300°K. This is similar to the dependence reported for artificial graphite.[19] It is not known whether the imper-

fections introduced by fast neutrons produce the same effects as those which may be found in graphite crystals. However, it may be significant that Washburn[3] found that his best specimens showed higher values for σ_c. Thus, if the measurements made by Krishnan and Ganguli and by Dutta are correct, it may be that their crystals contain more imperfections. It is unfortunate that Dutta's measurements of the effect of temperature on σ_a and σ_c have not been carried into the significant region below 90°K. However, if his data are plotted on the graphs presented here, his curve for σ_a falls somewhat above the data shown here, and this is interpreted as indicating more scattering in his crystals. If the minimum found here in the temperature variation of σ_c is general, his results for σ_c are entirely deceptive.

There is not enough information to interpret the few low-temperature data reported here for natural graphite crystals. The temperature dependence of the resistivity found here must involve a contribution from scattering by imperfections and possibly impurities. It seems likely that much of the a-axis resistance found below 10°K, where the power dependence decreases, is due to these contributions. However, these contributions must also make enough contribution to the region 15°K to 70°K to give an apparent power dependence lower than that which would be found if one had more "perfect" graphite crystals. Thus, without further experimental information, it does not seem wise to compare these results with the results of Wallace's[20] theoretical study.

ACKNOWLEDGMENTS

[17] H. Ott, Ann. Physik **85**, 86 (1928).
[18] Hennig, Fuchs, and Montet (unpublished).
[19] Reynolds, Hemstreet, and Leinhardt, Phys. Rev. **91**, 1152 (1953).

[20] P. R. Wallace, Phys. Rev. **71**, 634 (1947).

FIG. 1. Photomicrograph of typical graphite crystals of the sort used in the measurements described here. The scale is millimeters.